Double-Layer Transmitarray Antenna based on Coupled Rectangular Loops at 9.8 GHz

Mustika Fitriana Dewi[1], Umaisaroh[1], Ahmad Firdaus[1], Said Attamimi[1], Muzammil Jusoh[2], Mudrik Alaydrus[1]

[1]Department of Electrical Engineering, Universitas Mercu Buana, Jakarta, Indonesia,
[2]Advanced Communication Engineering, Centre of Excellence, Faculty of Electronic Engineering Technology, Universiti Malaysia, Perlis, Malaysia
mudrikalaydrus@mercubuana.ac.id

Abstract: Transmitarray is a high gain antenna suitable for various applications such as satellite communications, automotive radars, and future cellular communication systems. In order to attain a high gain, the diverging rays are focused by compensating the phase of the rays. The unit cell elements in the transmitarray are responsible for passing the electromagnetic energy appropriately to compensate for the phase excesses. A transmitarray antenna with 7×7 elements was designed and realized at a frequency of 9.8 GHz. The unit cell element consists of two coupled open rectangular resonator loops to sharpen the transmission stop region, broadening the phase range compared to a single open rectangular resonator loop. The fabrication process uses the Rogers Duroid 4003C substrate. A gap of 4 mm separates the substrate layers. The antenna has a gain of 18.5 dBi and an aperture efficiency of 31.7%.

Keywords: Coupled Rectangular loop; Multilayer; Transmitarray; X-Band

1. Introduction

The transmitarray antenna is a high-gain antenna exploiting the advantages of planar array structure and simple ray optical techniques. A feed antenna, usually a horn, radiates electromagnetic waves in form of rays with spherical phase fronts. The phase of the rays in this direction must be adjusted to a constant value, in order to collimate the rays to a given direction. A planar array is responsible for compensating the phase excess or shortage in each inspected ray through each dedicated unit cell element. In the past, there are various units cell structures with different geometrical shapes and dimensions to fulfill this goal [1]. In recent times, the design of transmitarray antennas becomes state of the art. The researchers realized significant advancement, especially in wideband/dual band applications, beamsteering, beamforming, and exploiting the uniqueness of metamaterial structures [2].

One of the essential things in designing the transmitarray antennas is the ability of the array structure to allow through the electromagnetic waves. The transmission factor of the electromagnetic waves through the array structure must have a high value (for example, better than -1 dB) and a broad phase range to compensate the phase difference between the rays. In [3], an analytical study of the effect of the number of layers on the phase range was conducted. The results showed that there is a limit of the phase range to be achieved from an analytical view. The more the number of layers used, the wider the phase range obtained. The authors in [4] gave results of 360° phase range with four layers structure of a total thickness of 0.75λ. The transmitarray consists of cross slots in metallic sheets as the unit cell elements. A two layers transmitarray with Malta crosses was proposed in [5]. The Malta crosses are connected through four via holes; this antenna achieves a gain of 33 dBi and an aperture efficiency of 40%. The researchers in [6] proposed a metal-only C-shaped unit cell for application at 29.5 GHz. The transmitarray consists of three layers with a total thickness of 0.59λ, a gain of 29.9 dBi, and an aperture efficiency of 50.9%.

Previously, a transmitarray antenna has been suggested in [7]. The antenna consists of three layers that work at the X-Band frequency with 537 spiral dipole elements. The gain of the transmitarray antenna is 28.9 dBi at a frequency of 11.3 GHz. In [8], a triple-layer transmitarray

Received: September 22th, 2021. Accepted: August 21st, 2022
DOI: 10.15676/ijeei.2022.14.3.2

antenna has been implemented. The shape of the unit cell patch is a split diagonal cross element with 9×9 elements. This antenna works at the frequency of 12.5 GHz and has a measured gain of 18.9 dBi. In [9], a triple-layer dual-mode meta-atom wherein an H-shaped structure at X-Band frequency has been implemented. The quad-beam transmitarray consists of 25×25 elements and has a peak gain of 18.8 dBi at 9.6 GHz. Another three layers transmitarray antenna was presented in [10]. The unit cell combined a cross-slot configuration and a double square ring. The gain of the antenna at 12.4 GHz was 25.8 dBi. The transmitarray consisted of 233-unit cell elements etched in a circular shape with a diameter of 221 mm and a total thickness of 15 mm (0.62λ).

In this work, the proposed transmitarray antenna will be designed and implemented that works at the frequency of 9.8 GHz and has a gain more than 18 dBi. The parameters observed from this antenna design are the good transmission factor value at the working frequency and the gain parameter generated by the antenna. The proposed unit cell design begins with an open rectangular loop.

2. Transmitarray and Design of Unit Cell Element

A. Transmitarray as Rays Focusing Electromagnetic Structure

A transmitarray antenna is a focusing structure that converts an electromagnetic wave with spherical phase fronts into a wave with planar phase fronts. Figure 1 shows spherical phase fronts leaving a feed, a horn antenna, or other antenna types. After passing the transmitarray structure, the rays become parallel. In this way, we obtain a gain-enhanced antenna. We discretize the transmitarray structure into small rectangular unit cell elements as given in Figure 1. The unit cell elements are responsible for compensating the phase difference of the rays so that after passing the transmitarray structure, the rays have the same phase delays and the phase fronts become planar.

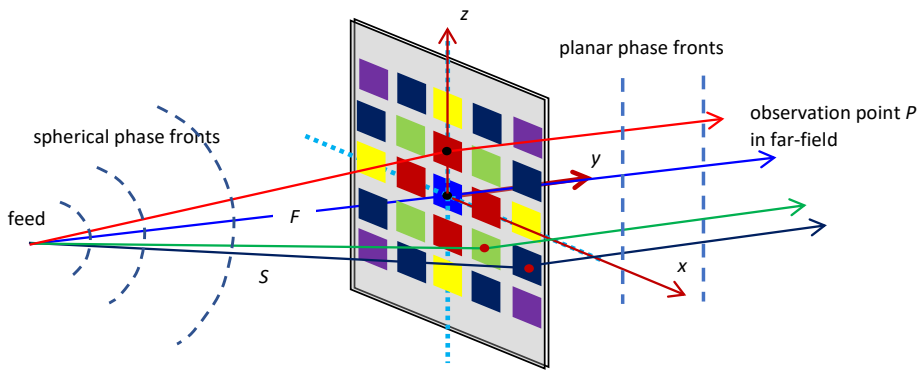

Figure 1. Transmitarray antenna converts spherical phase front into planar phase front.

In this work, we used the substrate Rogers RO4003 (relative permittivity ε_r = 3.55, tan δ = 0.0027) with a thickness of 0.51 mm for designing the transmitarray. The guided wavelength of electromagnetic waves at the working frequency of 9.8 GHz is around λ_g =18.2 mm and the wavelength in free space is λ_o =30.6 mm.

B. Open Rectangular Loop on a Substrate Layer

In order to design the phase-compensating elements, we propose a quasi-periodic structure. The structure consists of small elements called unit cell elements. In this work, we discretize the transmitarray into small rectangular unit cell elements, which have the size of $0.5\lambda_o \times 0.5\lambda_o$ =15.3 mm × 15.3 mm. In each element, we design an open rectangular loop as a resonating element with a side length of *L*×*L* and a width of *h*. The opening of the loop is *s*. Figure 2a) shows a unit cell element. The symmetric resonator has a fixed opening with a fixed value s=0.5

mm and a fixed width h=0.5 mm. The values are chosen small to keep the generated capacitance small, and to avoid lateral electric current along the loop. We model the loop as a perfectly electric conductor; we use the periodic boundary conditions (master and slave boundary conditions) for four lateral sides and two Floquet ports to analyze the unit cell element's reflection and transmission characteristics, as given in Figure 2b).

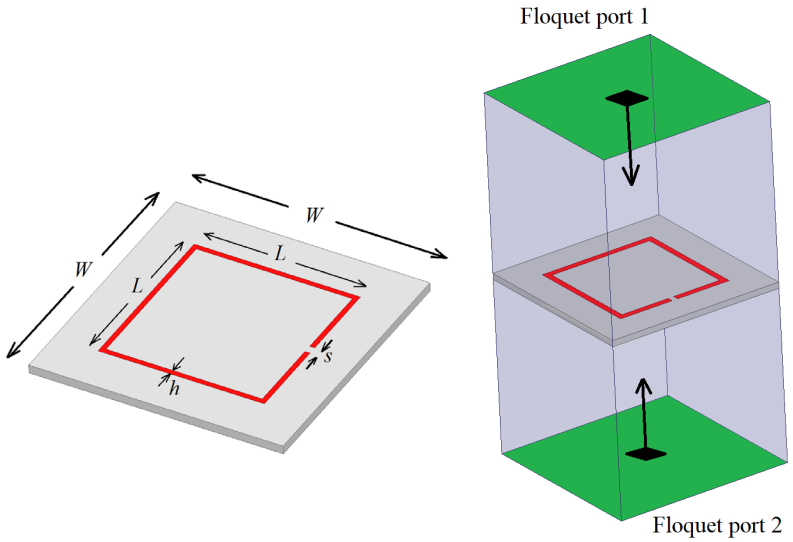

Figure 2. a) Open rectangular loop as unit cell element, W =15.3 mm, h = 0.5 mm, s = 0.5 mm and 4 mm ≤ L ≤ 14 mm, b) Modeling the unit cell in a periodic boundary condition.

At first step, in this work, we keep the values W = 15.3 mm, h = 0.5 mm, and s = 0.5 mm constant and do a variation of the side length L from 4 mm to 14 mm to inspect possible high phase variation for compensating excess phases of the wave rays due to different distances from the horn to the transmitarray.

From the simulation results in Figure 3, the unit cell element shows resonance for around L = 10 mm, the transmission factor goes to a minimal value. For around 4 mm ≤ L ≤ 7 mm, the magnitude of the transmission factor is more than -0.5 dB, which through the following calculation

$$\% \text{ transmitted energy} = 10^{S21/10} \text{ x } 100\% = 10^{-0.5/10} \text{ x } 100\% = 89\% \quad (1)$$

means 89% of the energy is transmitted. The achievable phase difference is around 12°. By allowing only 80% to be transmitted (the magnitude more than -1 dB), we get around 19° phase difference.

Although for 12.5 mm ≤ L, we find high transmission again with a higher phase difference (almost 360°), this condition is practically useless due to the unavailability of the phase value in the middle. This slight maximal phase difference of this unit cell element restricts the flexibility to design transmitarray antennas.

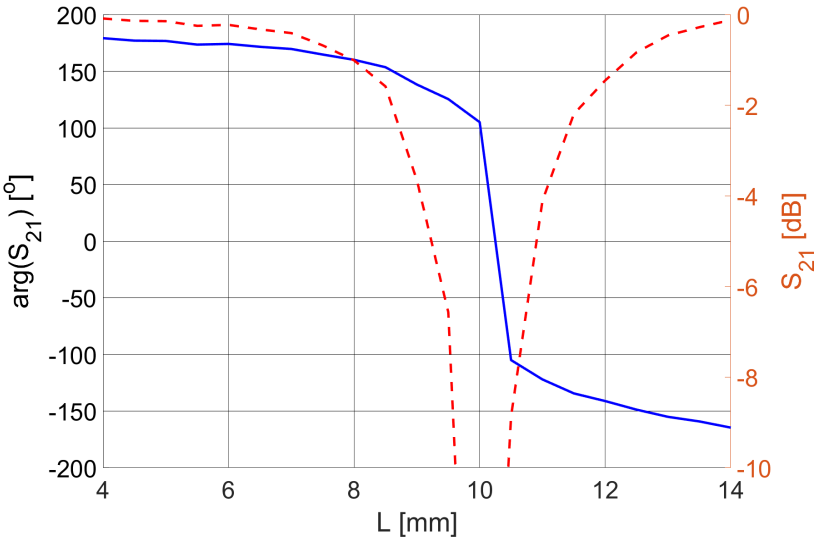

Figure 3. The magnitude (dashed line) and the phase of the transmission factor S_{21} (solid line) as a function of the side length *L*.

C. Coupled Open Rectangular Loops on two Substrate Layers

Next, we attempted to enhance the phase characteristics of the unit cell element by using two substrate layers. We can make an additional variation in the distance between the layers in this design, and we designate it as the gap. In this work, we observed the position of the loop breakings. Figure 4a) shows the position of breakings on the same side, which observes the electric coupling between the loops, whereas Figure 4b) gives the case for the position on the opposite side, representing hybrid couplings. The magnitude and phase of the transmission factor, however, are similar.

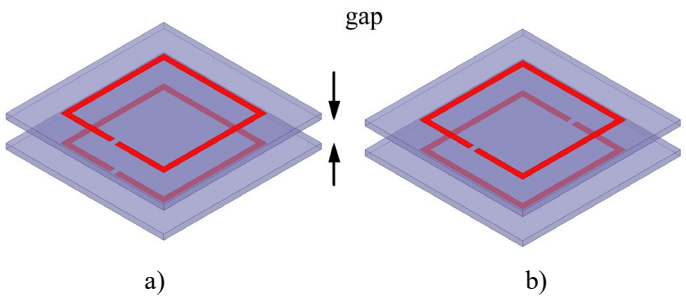

Figure 4. Coupled open rectangular loops in different layers as unit cell elements, a) loop break on the same side, b) loop break on the opposite side.

From the filter theory [11], we use coupled resonator structures to enhance the selectivity of the filters. In Figure 5a) we find, the bandstop region around L = 10 mm shows strong steepness, especially for gap = 2 mm, 3 mm, and 4 mm. Figure 5b) gives the phase of the transmission factor S21 through the unit cell element. Allowing a reduction of transmission by 0.5 dB, which means 89% energy is transmitted, we get a 76° phase difference for gap = 3 mm, 32° for gap = 4 mm, 42° for gap = 5 mm and 45° for gap = 6 mm. If we sacrifice the transmitted energy by -1 dB, or only 80% transmission energy, we get a 76° phase difference for gap = 3 mm, and around 92° for gap = 4 mm.

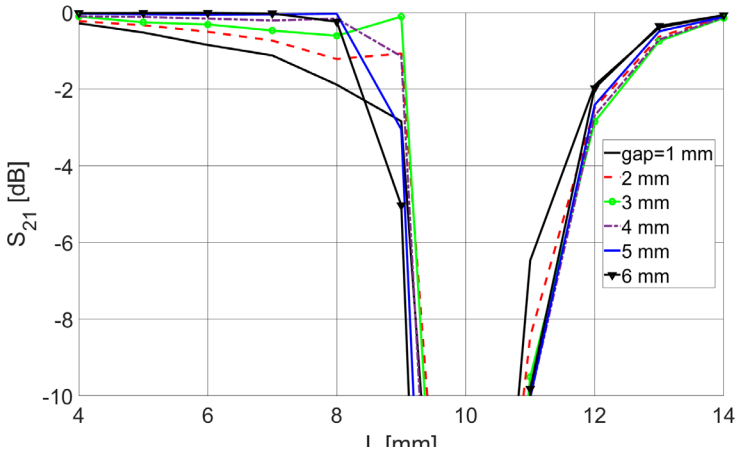

(a)

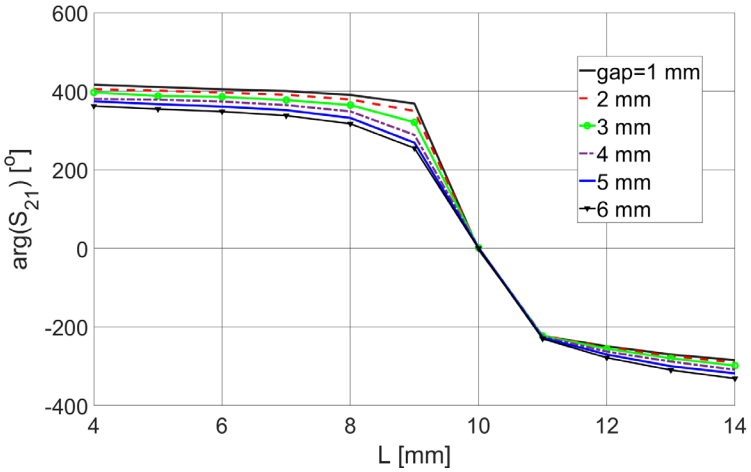

(b)

Figure 5. a) Magnitude in dB, b) Phase in degrees of the transmission factor as a function of the side length of the loop (L) and the separation between the layers (gap).

D. Strategy for High Gain

In this section, we did preliminary study for achieving the gain of the transmitarray at around 18 dBi. From the theory [12], we know that the maximal theoretical gain can be obtained from

$$G_{ideal} = \frac{4\pi A}{\lambda^2}, \quad (2)$$

A is the area of the transmitarray, which is equal to $NW \times NW$, and N^2 is the total number of the unit cells. Due to the limited efficiency of the illumination by the horn, the real obtainable gain is usually much smaller. By introducing the efficiency factor (or aperture efficiency) ε_{Ap}, the real obtainable gain becomes

$$G_{real} = \varepsilon_{Ap} \frac{4\pi A}{\lambda^2} \quad (3)$$

The value of the aperture efficiency in a transmitarray antenna, referred to the available literature, ranges from 10% to 50%.

In respect of this condition, we did some preliminary studies, and calculated some cases as given in Table 1.

Table 1. Prediction of real obtainable gain due to aperture efficiency

N	$G_{ideal} = 4\pi A/\lambda^2$	ε_{Ap}	$G_{real} = \varepsilon_{Ap} G_{ideal}$
3	28.27 ≡ 14.5 dBi	20%	5.6 ≡ 7.5 dBi
		50%	14.1 ≡ 11.5 dBi
4	50.27 ≡ 17.0 dBi	20%	10.0 ≡ 10.0 dBi
		50%	25.1 ≡ 14.0 dBi
5	78.54 ≡ 18.95 dBi	20%	15.7 ≡ 11.96 dBi
		50%	39.3 ≡ 15.9 dBi
6	113.1 ≡ 20.5 dBi	20%	22.6 ≡ 13.5 dBi
		50%	56.5 ≡ 17.5 dBi
7	153.94 ≡ 21.88 dBi	20%	30.8 ≡ 14.9 dBi
		50%	76.97 ≡ 18.9 dBi
8	201.1 ≡ 23.03 dBi	20%	40.2 ≡ 16.0 dBi
		50%	100.53 ≡ 20.0 dBi

In respect to table 1, we proposed a transmitarray with 7x7 arrangement to obtain a gain of around 18 dBi.

3. Designing Transmitarray Antenna

Based on the transmission characteristics of the unit cell element, we design the complete transmitarray antenna by arranging the unit cell element with the appropriate side length to obtain the needed phase compensation for each electromagnetic ray.

A. Calculating the Phase Distribution on the Transmitarray Structure

We calculated first the phase of the individual rays of the electromagnetic wave at the position of the impact point on the transmitarray. The rays emanate radially from a point source located at a distance r_0 from the transmitarray, and after the transmission through the double-layered transmitarray, we focus the wave to the y-direction as given in Figure 6.

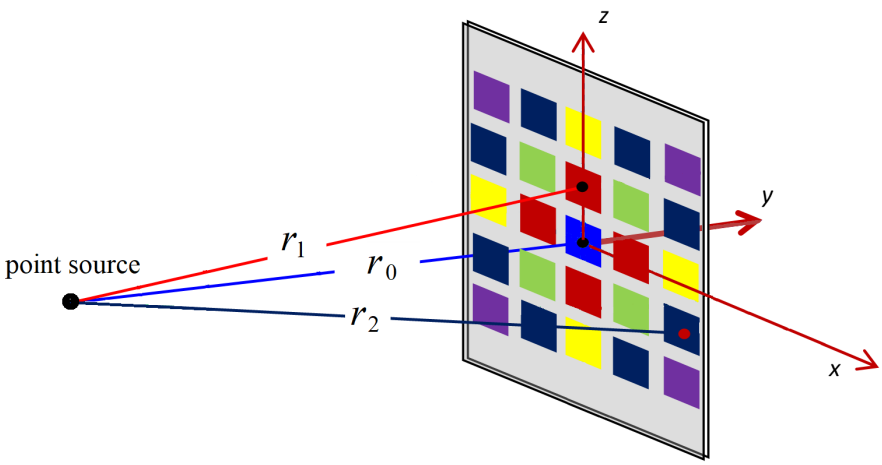

Figure 6. Calculating the phase of the rays on the impact points.

Due to the position of the source on the axis of the system, the distance from the source to the midpoint (x=0,y=0,z=0) is the smallest distance, the ray on this point has the phase

$$\varphi_0 = -\frac{2\pi}{\lambda} r_0 \tag{4}$$

The phase of the rays in other impact points, can be calculated through all distances from the point sources to the midpoints of the unit cells via Pythagoras'rule. If we norm all phases to the phase of the ray on the center, we have negative phase excesses for all unit cell. For any unit cell *i* in the transmitarray, the phase becomes

$$\varphi_i = -\frac{2\pi}{\lambda}(r_i - r_0) \quad (5)$$

Each unit cell element must compensate the excess phase due to this propagation delay of each ray. Figure 7 gives the phase distribution for each element. The values are positive compared to the phase for ray with minimal propagation delay, i.e., the central unit cell element.

80.1	58	44.7	40.3	44.7	58	80.1
58	35.8	22.4	18	22.4	35.8	58
44.7	22.4	8.99	4.5	8.99	22.4	44.7
40.3	18	4.5	0	4.5	18	40.3
44.7	22.4	8.99	4.5	8.99	22.4	44.7
58	35.8	22.4	18	22.4	35.8	58
80.1	58	44.7	40.3	44.7	58	80.1

Figure 7. Distribution of phase (in degrees) on each unit cell element for compensating the phase excess due to longer propagation for the beam direction to the positive z-axis.

B. Designing the Full Transmitarray and Fabrication

Based on the phase on the transmitarray needed for compensating the propagation delay as shown in Figure 7, we can use the relationship between the phase of the transmission factor and the geometry parameter, in this case, the side length of the open-loop resonator. According to Figure 5b), we listed the curves for three gaps between the layers for the geometry parameter *L* from 4 mm to 9 mm as given in Table 2. Table 2 offers a kind of lookup table for designing the full transmitarray for simulation and measurement purposes.

Table 2. Phase Difference in Respect to *L* = 9 mm

***L* in mm**	**80% transmission**	**89% transmission**	**80% transmission**
	gap = 2mm	**gap = 3 mm**	**gap = 4 mm**
4	55.4	76.0	91.6
5	51.7	66.9	89.8
6	47.0	64.6	84.9
7	41.2	56.3	75.8
8	29.2	43.7	59.9
9	0	0	0

We see in Table 2, that the 80% transmission (-1dB S_{21}) with a gap of 4 mm is able to cover the whole required phase range as given in Figure 7. The bigger loops dominate in the mid part of the transmitarray (long L), whereas the smaller loops will be in the edge region of the transmitarray (short L).

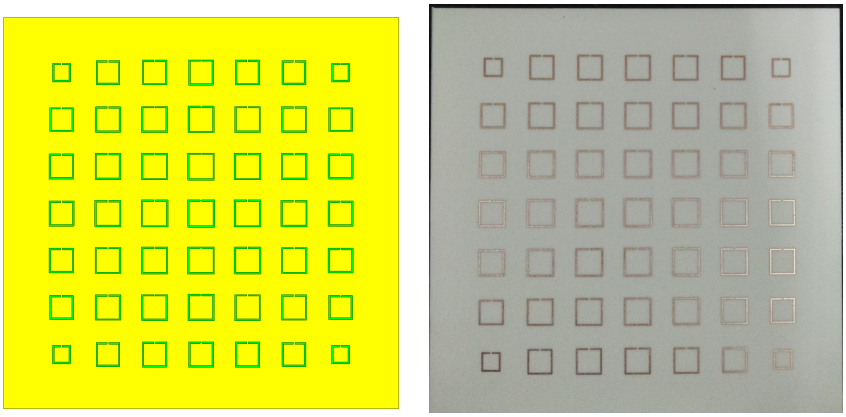

a) b)

Figure 8. a) Simulation model of the transmitaray, b) fabricated transmitarray antenna, total dimension 129 mm × 129 mm.

For further analysis, we use the information for the gap distance of 4 mm, allowing the condition that only 80% of the transmitted energy, or reduction of propagation path by 1 dB. By comparing the phase distribution in Figure 7 and the data in Table 2 for gap = 4 mm, we design the full transmitarray as given in Figure 8a). Any phase value not available in Table 2 can be interpolated. We fabricated this model in RO4003 substrate as given in Figure 8b).

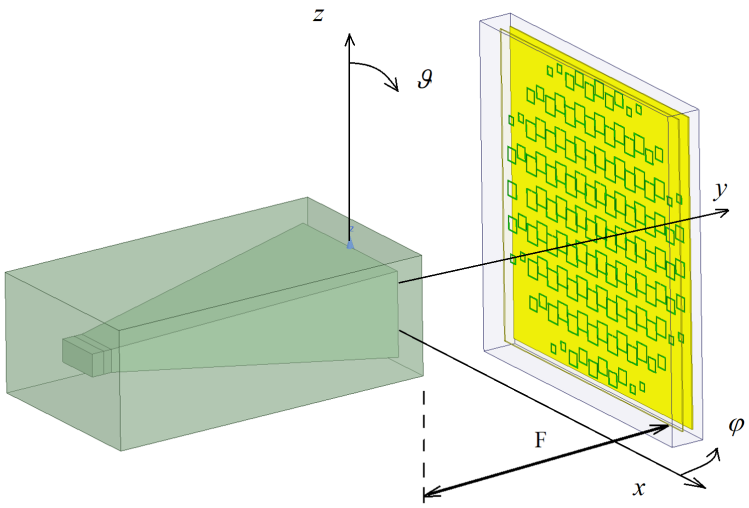

Figure 9. Simulation model: horn antenna and transmitarray separated by the distance F.

4. Results and Discussion

For calculation purposes, we modeled the transmitarray antenna with a feed horn in HFSS environment. The computer model of the complete antenna system is presented in Figure 9. As illustrated in the figure, the feed horn and the transmitarray are surrounded by radiation boundary boxes. The boxes act as Huygen's surface outward, so that the coupling interaction between the feed horn and the transmitarray was numerically considered by an integral equation approach. With this model, we can vary the distance from transmitarray to the horn aperture F to study the effect of the feed position on the calculated gain of the antenna system without any additional computer memory requirements.

Figure 10 gives the magnitude of the surface current density on the front layer of the transmitarray. We see, that the magnitude of the surface current density for the distance F=125 mm (left picture) is higher and distributed on almost whole transmitarray than for the distance F=25mm (right picture). Together with the radiation characteristics of the horn antenna, this current distribution leads to the focusing of the energy to the main direction (positive y axis according to Fig. 9). The higher and more evenly distributed surface current density for F=125 mm generates a gain of around 18.4 dBi, whereas the in the mid concentrated surface current density for F=25 mm generates a rather smaller gain of around 12.5 dBi. The more evenly distributed surface current density indicates a high value of aperture efficiency, what we will see next in discussing the gain of the antenna.

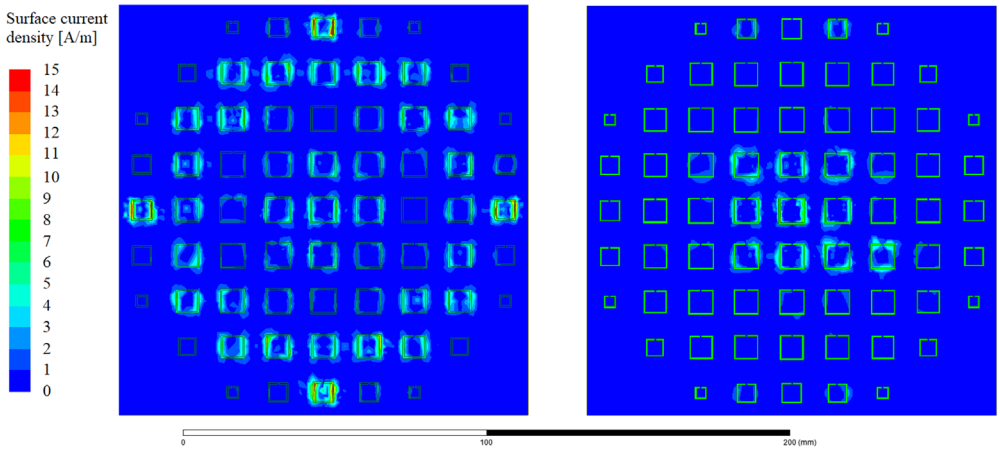

Figure 10. Magnitude of the surface current density for F=125 mm, case: higher gain (left) and for F=25 mm, case: lower gain (right).

In order to measure the gain and the radiation pattern of the antenna, we built the measurement testbed as shown in Figure 11. The transmitarray antenna as the antenna under test (AUT) is separated from the testing antenna at a distance R = 200 cm, which is adequate to fulfill the far-field condition for an antenna dimension up to 173 mm.

The AUT was positioned on a rotating table to study the horizontal and vertical radiation pattern of the antenna. Because we did the measurement not in an anechoic chamber, we let pyramidal absorbing structures in several critical positions. We calculated the gain of the antenna system as a function of the feed distance F and compared the simulation and measurement results as given in Figure 12. The gain of the AUT increases with the feed distance F from 20 mm to around 70 mm, and then by increasing the feed distance, the gain value fluctuates between 17 dBi and 18 dBi. It seems the effect of the phase compensation works effectively at the feed distance of around 80 mm.

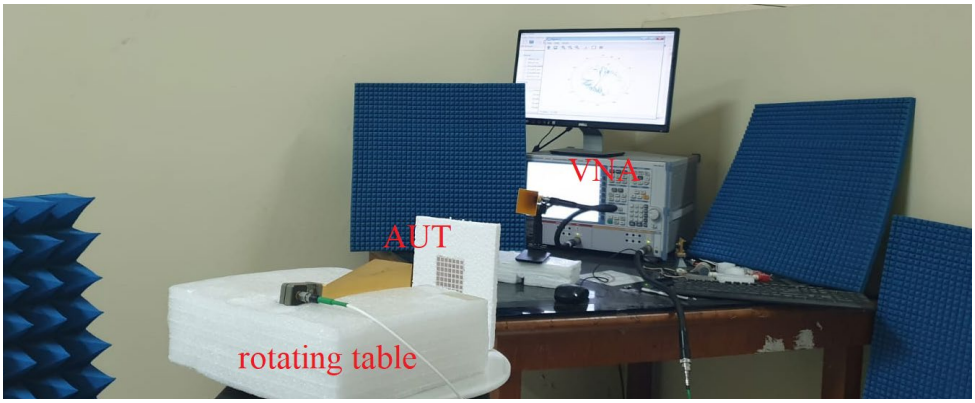

Figure 11. Measurement testbed with a distance between antennas R = 200 cm.

At small distances F, it seems, the horn illuminates only the middle part of the transmitarray effectively. With increasing distances, the illuminated region becomes larger, the gain increases continually. Beginning at around F=80 mm, the illumination becomes complex, not only the illuminated region increases, but also the complex-valued surface current density is distributed on a very large region more than four times of the wavelength (129 mm x 129 mm = $4.2\lambda \times 4.2\lambda$), it develops constructive and destructive interferences from each surface current contribution. The gain fluctuates to high values for constructive combinations then to low values for destructive combinations.

At very large distances at around F > 140 mm, the gain descreases due to spill over of the illumination, many parts of the rays surpass the transmitarray and never come to the receiver.

The measured gain verifies the calculated gain; we see the tendency of the value. According to Figure 12, we find the maximal calculated gain at around 18.4 dBi and a maximal measured gain at around 18.5 dBi by a distance of 130 mm from the feed to the transmitarray. With this measured gain and the physical dimension of the antenna of 129 mm ×129 mm, the aperture efficiency of the designed antenna becomes 31.7%.

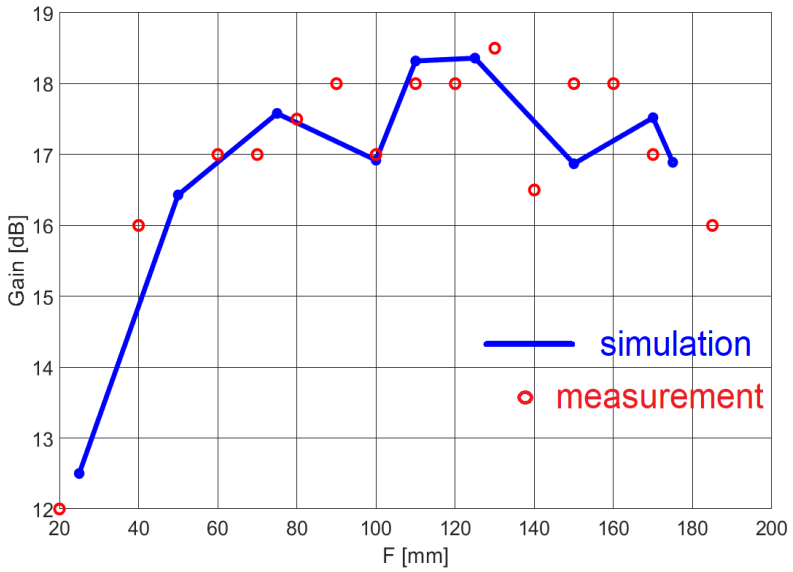

Figure 12. Gain of the transmitarray antenna as a function of the distance between horn and the transmitarray at 9.8 GHz, simulation (blue solid line), measurement (red circles).

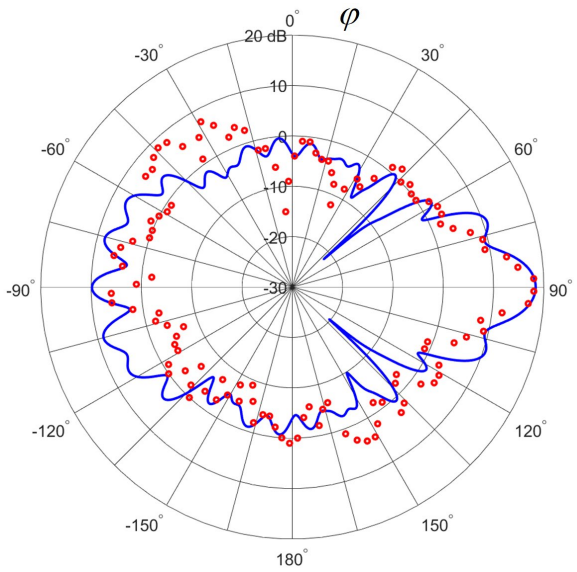

a)

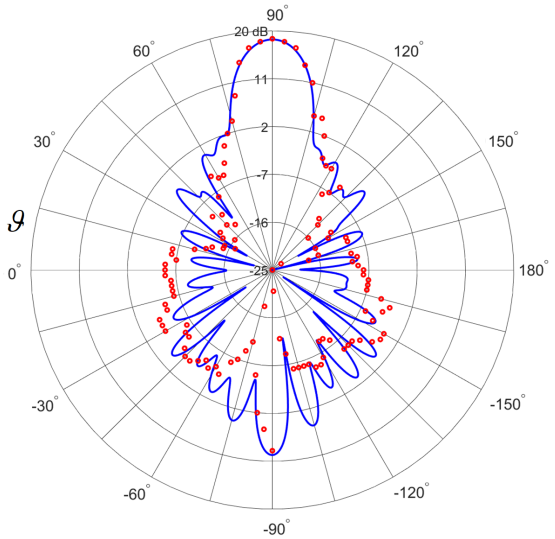

b)

Figure 13. Comparison of calculated (solid blue) and measured (dotted red) radiation diagram a) horizontal ($\vartheta = 90^o$, xy plane in Fig. 9), b) vertical ($\varphi = 90^o$, yz plane in Fig. 9). The simulation and measurement were performed at the frequency of 9.8 GHz and F = 130 mm.

Figure 13a) gives the comparison of the calculated and measured horizontal radiation diagram, which is the xy plane in Fig. 9. The calculated and measured radiation diagram confirms the main beam direction to φ = 90° according to the convention in Figure 9. In contrast, the results confirm a negative effect of the transmitarray antena, that the back lobe to direction φ = -90° increases to a value of 10 dB below the main beam, which may be unacceptable for many applications. The measurements confirm the many side lobes almost all around the horizontal plane. We see a similar condition for the vertical radiation diagram (yz plane) as given in Figure 13b) with a smaller first side lobe.

In Table 3, we see the comparison of the results with other publications. There are several models and approaches used to enhance the aperture efficiency of the antennas. The designs are differentiated between slot and patch structures, which resonate with certain specific bandstop or bandpass-characteristics. Moreover, we can divide the designs in implementation of vias or not. The antenna gains reported depend on significantly on the ratio between the dimension of the antenna to the working wavelength, so that it is more precisely to compare the aperture efficiency of each antenna. As we can see in Table 3, all models with vias achieve higher aperture efficiency. This work offers moderate aperture efficiency but easier fabrication than vias structure. We could compare our results with results in [4], [8], and [16], which studied almost the similar frequency region (X-Band). Our result shows higher aperture efficiency compared than [4] and [8], but lower than [16]. We used only 7x7=49 unit cells in comparison with 341 unit cells in [16].

Table 3. Comparison of important results between this work and previous research.

Ref.	Frequency [GHz]	Gain [dBi]	Design/Technique	Aperture efficiency [%]	Number of layers	Thickness
[4]	11.3	23.76	Cross slot	14.2	4	0.75λ
[5]	20	33	Malta cross-connected by 4 vias	40	2	0.11λ
[8]	12.5	18.9	Square ring intersected by split diagonal cross	20.9	2	0.52λ
[13]	18	29.2	Cross patches with stub and vias	51.4	2	0.12 λ
[14]	18.5	22.5	Double rectangular ring and Jerusalem slot	46.0	3	0.15 λ
[15]	6.1	20.1	Rectangle Ring Slot	27.0	3	0.61 λ
[16]	10	21.9	Cross slot and T-slot	36.0	2	0.03λ
[17]	21	29.4	Cross spiral dipole and vias	40	2	0.07λ
[18]	60	23.9	Rotated squared patches with a via	17	3	0.10 λ
This work	9.8	18.5	Coupled open rectangular loop	31.7	2	0.18 λ

5. Conclusion

The paper presents a double-layer transmitarray antenna with a gap of 4 mm between the substrates. The unit cell element consists of two coupled open rectangular resonator loops to sharpen the transmission stop region, broadening the phase range compared to a single open rectangular resonator loop. The antenna works at the frequency of 9.8 GHz; it has a maximal calculated gain of 18.4 dBi and a maximal measured gain of 18.5 dBi and an aperture efficiency of 31.7%.

6. Acknowledgment

The authors would like to thank Kemendikbudristek and Universitas Mercu Buana for supporting this research.

7. References

[1]. K. Narayanasamy, G. N. A. Mohammed, K. Savarimuthu, R. Sivasamy, and M. Kanagasabai, "A comprehensive analysis on the state-of-the-art developments in reflectarray, transmitarray, and transmit-reflectarray antennas*," International Journal of RF and Microwave Computer-Aided Engineering*, vol. 30, no. 9. John Wiley and Sons Inc., Sep. 01, 2020. doi: 10.1002/mmce.22272.

[2]. J. R. Reis, M. Vala, and R. F. S. Caldeirinha, "Review paper on transmitarray antennas," IEEE Access, vol. 7, pp. 94171–94188, 2019, doi: 10.1109/ACCESS.2019.2924293.

[3]. A. H. Abdelrahman, A. Z. Elsherbeni, and F. Yang, "Transmission phase limit of multilayer frequency-selective surfaces for transmitarray designs," *IEEE Transactions on Antennas and Propagation*, vol. 62, no. 2, pp. 690–697, 2014, doi: 10.1109/TAP.2013.2289313.

[4]. A. H. Abdelrahman, A. Z. Elsherbeni, and F. Yang, "Transmitarray antenna design using cross-slot elements with no dielectric substrate," *IEEE Antennas and Wireless Propagation Letters*, vol. 13, pp. 177–180, 2014, doi: 10.1109/LAWP.2014.2298851.

[5]. W. An, S. Xu, F. Yang, and M. Li, "A Double-Layer Transmitarray Antenna Using Malta Crosses with Vias," *IEEE Transactions on Antennas and Propagation*, vol. 64, no. 3, pp. 1120–1125, Mar. 2016, doi: 10.1109/TAP.2015.2513427.

[6]. T. K. Pham, A. Clemente, E. Fourn, F. Diaby, L. Dussopt, and R. Sauleau, "Low-cost metal-only transmit array antennas at Ka band," vol. 18, no. 6, pp. 1243–1247, 2019, doi: 10.1109/LAWP.2019.2913571ï.

[7]. A. H. Abdelrahman, A. Z. Elsherbeni, and F. Yang, "High-gain and broadband transmitarray antenna using triple-layer spiral dipole elements," *IEEE Antennas and Wireless Propagation Letters*, vol. 13, pp. 1288–1291, 2014, doi: 10.1109/LAWP.2014.2334663.

[8]. J. Yu, L. Chen, J. Yang, and X. Shi, "Design of a Transmitarray Using Split Diagonal Cross Elements with Limited Phase Range," *IEEE Antennas and Wireless Propagation Letters*, vol. 15, pp. 1514–1517, 2016, doi: 10.1109/LAWP.2016.2517019.

[9]. H. X. Xu, T. Cai, Y. Q. Zhuang, Q. Peng, G. M. Wang, and J. G. Liang, "Dual-Mode Transmissive Metasurface and Its Applications in Multibeam Transmitarray," *IEEE Transactions on Antennas and Propagation*, vol. 65, no. 4, pp. 1797–1806, Apr. 2017, doi: 10.1109/TAP.2017.2673814.

[10]. C. Tian, Y. C. Jiao, G. Zhao, and H. Wang, "A Wideband Transmitarray Using Triple-Layer Elements Combined with Cross Slots and Double Square Rings," *IEEE Antennas and Wireless Propagation Letters*, vol. 16, pp. 1561–1564, 2017, doi: 10.1109/LAWP.2017.2651027.

[11]. D. W. Astuti, Juwanto, and M. Alaydrus, "A bandpass filter based on square open loop resonators at 2.45 GHz," in 2013 3rd *International Conference on Instrumentation, Communications, Information Technology and Biomedical Engineering (ICICI-BME)*, Nov. 2013, pp. 147–151. doi: 10.1109/ICICI-BME.2013.6698482.

[12]. C. A. Balanis, Antenna Theory: Analysis and Design, 4th ed., Wiley, 2016.

[13]. X. J. Yi, T. Su, B. Wu, J. Z. Chen, L. Yang, and X. Li, "A Double-Layer Highly Efficient and Wideband Transmitarray Antenna," *IEEE Access*, vol. 7, pp. 23285–23290, 2019, doi: 10.1109/ACCESS.2019.2893608.

[14]. X. Lv, Z. Han, X. Jian, Y. Zhang, and Q. Chen, "A wideband transmitarray using triple-layer elements with reduced profile," *IEICE Electronics Express*, vol. 17, no. 1, Jan. 2020, doi: 10.1587/elex.16.20190678.

[15]. X. Zhong, L. Chen, Y. Shi, and X. Shi, "Design of Multiple-Polarization Transmitarray Antenna Using Rectangle Ring Slot Elements," *IEEE Antennas and Wireless Propagation Letters*, vol. 15, pp. 1803–1806, 2016, doi: 10.1109/LAWP.2016.2537386.

[16]. C. Tian, Y. C. Jiao, and G. Zhao, "Circularly Polarized Transmitarray Antenna Using Low-Profile Dual-Linearly Polarized Elements," *IEEE Antennas and Wireless Propagation Letters*, vol. 16, pp. 465–468, 2017, doi: 10.1109/LAWP.2016.2583486.

[17]. X. Yi, T. Su, X. Li, B. Wu, and L. Yang, "A Double-Layer Wideband Transmitarray Antenna Using Two Degrees of Freedom Elements Around 20 GHz," *IEEE Transactions on Antennas and Propagation*, vol. 67, no. 4, pp. 2798–2802, Apr. 2019, doi: 10.1109/TAP.2019.2893265.

[18]. H. Kaouach, L. Dussopt, J. Lanteri, T. Koleck, and R. Sauleau, "Wideband low-loss linear and circular polarization transmit-arrays in V-Band," *IEEE Transactions on Antennas and Propagation*, vol. 59, no. 7, pp. 2513–2523, Jul. 2011, doi: 10.1109/TAP.2011.2152331.

Mustika Fitriana Dewi is a researcher from the Research Center of Electronics at the National Research and Innovation Agency (BRIN) of Indonesia. She received her bachelor's degree in Electrical Engineering from Universitas Mercu Buana, Jakarta. She spent 3 years working as Network Engineer at PT. Mora Telematika Indonesia before joining BRIN in 2021. Currently, she is a member of the Optoelectronics research group in the field of optical communications and fiber optic sensor systems. She can be reached through email: mustika.fitriana.dewi@brin.go.id.

Umaisaroh is currently a lecturer with the Department of Electrical Engineering in Universitas Mercu Buana, Jakarta, Indonesia. She received the B.A.Sc. degree in Telecommunication Engineering from Politeknik Elektronika Negeri Surabaya (PENS), in 2013, and Ph.D. degrees in electrical engineering from Institut Teknologi Sepuluh Nopember (ITS), in 2019. She has been studied on HF skywave communications in equatorial regions. Her research interests include radio propagation, wireless communication, millimeter wave, and antenna system.

Ahmad Firdausi was born in Madiun, Indonesia, on July 15, 1990. He is currently studying Ph.D. at the Sepuluh Nopember Institute of Technology (ITS) Surabaya, Indonesia. From 2017 until now, he has been a lecturer at Universitas Mercu Buana, Jakarta, Indonesia. His research interests include Wireless Sensor Networks, Next Generation Networks, Electromagnetic Wave Propagation, Antenna Design, and Telecommunication Systems.

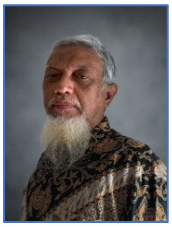

Said Attamimi is a senior lecturer at Department of Electrical Engineering, Universitas Mercu Buana. He holds a bachelor degree from Institut Teknologi Bandung and a master degree from Universitas Indonesia, both in Electrical Engineering.

Muzammil Jusoh is an Associate Professor which is currently a Research Fellow of Advanced Communication Engineering (ACE) Centre of Excellence (CoE) in UniMAP. Experience as RF and Microwave Engineer with Telekom Malaysia Berhad (TM) company, from 2006 to 2009. He received the bachelor's degree in electrical-electronic and telecommunication engineering and the M.Sc. degree in electronic telecommunication engineering from Universiti Teknologi Malaysia (UTM), in 2006 and 2010, respectively, and the Ph.D. degree in communication engineering from Universiti Malaysia Perlis (UniMAP), in 2013. Has published over 240 articles in journals and proceedings. His research interests include antenna design, reconfigurable beam steering antennas, RFID, MIMO, UWB, wireless on-body communications and RF and microwave communication systems. A member of the IET

(MIET), the Antenna and Propagation Society (AP/MTT/EMC) Malaysia Chapter and Executive Committee of IEEE RFID Council.

Mudrik Alaydrus is Professor at Department of Electrical Engineering, Universitas Mercu Buana, Jakarta. He holds a Dr.-Ing degree in Electrical Engineering with specialization in Electromagnetics. From 1997 to 2002 he was a researcher at the chair of electromagnetics at University of Wuppertal, Germany. Since 2003, he has worked at Universitas Mercu Buana. His research areas are electromagnetics, microwave and millimeter waves as well as mathematical approachs for signal processing. Mudrik Alaydrus has more than 200 publications in journals and conferences, wrote four books in Transmission Lines, Antennas, Electromagnetic Fields and Microwave Engineering, all in Indonesian, and has been awarded two patents. He is a Senior Member of IEEE and member of Verein Deutscher Elektroingenieure (VDE) as well as member of Persatuan Insinyur Indonesia (PII). He was the chair of the Joint AP/MTT Indonesia Chapter. He can be contacted at email: mudrikalaydrus@mercubuana.ac.id.